Optical system design and integration of the Lunar Orbiter Laser Altimeter

Luis Ramos-Izquierdo,[1,*] V. Stanley Scott III,[2] Joseph Connelly,[1] Stephen Schmidt,[3] William Mamakos,[4] Jeffrey Guzek,[4] Carlton Peters,[5] Peter Liiva,[6] Michael Rodriguez,[6] John Cavanaugh,[7] and Haris Riris[2]

[1]NASA/Goddard Space Flight Center, Optics Branch, Greenbelt, Maryland 20771, USA

[2]NASA/Goddard Space Flight Center, Laser Remote Sensing Laboratory, Greenbelt, Maryland 20771, USA

[3]NASA/Goddard Space Flight Center, Electro-Mechanical Systems Branch, Greenbelt, Maryland 20771, USA

[4]Design Interface Inc., Finksburg, Maryland 21048, USA

[5]NASA/Goddard Space Flight Center, Thermal Systems Branch, Greenbelt, Maryland 20771, USA

[6]Sigma Space Corporation, Lanham, Maryland 20706, USA

[7]NASA/Goddard Space Flight Center, Laser and Electro-Optics Branch, Greenbelt, Maryland 20771, USA

*Corresponding author: Luis.A.Ramos-Izquierdo@nasa.gov

Received 15 January 2009; revised 16 April 2009; accepted 28 April 2009; posted 1 May 2009 (Doc. ID 106402); published 22 May 2009

The Lunar Orbiter Laser Altimeter (LOLA), developed for the 2009 Lunar Reconnaissance Orbiter (LRO) mission, is designed to measure the Moon's topography via laser ranging. A description of the LOLA optical system and its measured optical performance during instrument-level and spacecraft-level integration and testing are presented. © 2009 Optical Society of America

OCIS codes: 280.3640, 220.4830.

1. Introduction

The Lunar Orbiter Laser Altimeter (LOLA) is one of seven scientific instruments on board the Lunar Reconnaissance Orbiter (LRO) spacecraft [1], the first mission in NASA's Vision for Space Exploration, a plan to return to the Moon and then to travel to Mars and beyond. LRO is scheduled to launch in June 2009 and arrive at the Moon five days later for a one-year study from a nominal 50 km altitude circular mapping orbit. The goals of LRO are to select safe landing sites, identify lunar resources, and study how the lunar radiation environment will affect humans. LOLA will use laser ranging to measure the Moon's surface elevation, slope, and roughness and generate a three-dimensional map of the Moon; LOLA will also help identify permanently shadowed regions of the Moon where water ice might be present [2].

LOLA was designed and developed at NASA's Goddard Space Flight Center (GSFC) over a period of three years and delivered to the NASA/GSFC LRO team on April 2008 for spacecraft-level integration. The optical and optomechanical designs, optical materials and coatings, and many of the optical test setups used on LOLA are based on our previous work on the NASA/GSFC Mercury Laser Altimeter (MLA) instrument. A description of MLA's optical system and performance has been previously published [3]; to avoid duplication this paper will focus on the optical engineering aspects that are unique to LOLA.

2. Instrument Description

A comparison of the LOLA and MLA optical specifications is shown in Table 1. The main difference

0003-6935/09/163035-15$15.00/0

Table 1. Lunar Orbiter Laser Altimeter (LOLA) and Mercury Laser Altimeter (MLA) Optical Specifications

Laser transmitter	LOLA	MLA
# Laser oscillators	2	1
Wavelength (nm)	1064.3	1064.3
Pulse energy (mJ)	2.7	20
Pulse width (ns, FWHM)	6	6
Repetition rate (Hz)	28	8
Divergence (μrad, $1/e^2$ dia.)	100	80
# Beams/laser	5	1
Beam spacing (μrad)	500	n/a
Receiver optics	**LOLA**	**MLA**
# Receiver telescopes	1	4
Objective lens size (mm, dia.)	150	125
Collecting clear aperture (cm^2)	154	417
# Receiver FOV's	5	1
FOV (μrad, FWHM)	400	400
FOV spacing (μrad)	500	n/a
Fiber-optic coupled	Yes	Yes
Bandpass filter (nm, FWHM)	0.7	0.7
# Detectors	5	1
Detector type	SiAPD	SiAPD
Detector size (mm, dia.)	0.7	0.7

between MLA and LOLA is that MLA is a single channel instrument, while LOLA has multiple laser ranging channels: MLA has a single transmitted laser beam, four receiver telescopes (for increased collecting aperture area), and a single detector, while LOLA has five transmitted laser beams, a single, multiple FOV receiver telescope, and five detectors. LOLA can process the detector signals independently to generate five range measurements per laser shot; this approach increases coverage of the lunar surface and provides local slope data. Due to the difference in mapping orbits, 50 km for LOLA and up to 800 km for MLA, the laser transmitter output energy and receiver telescope collecting aperture requirements are very different for the two instruments. Another difference between MLA and LOLA is that MLA operates at a single wavelength (1064 nm), while LOLA operates at two wavelengths (1064 nm and 532 nm). LOLA will use the 1064 nm wavelength to map the Moon and the 532 nm wavelength for laser ranging from Earth to LRO [4] in order to improve the orbit determination of LRO to the level required to generate an accurate topographic map of the Moon.

Like MLA, LOLA is composed of two subassemblies connected by an electrical harness: the Optical Transceiver Assembly (OTA) and the Main Electronics Box (MEB). An assembly drawing of the LOLA OTA is shown in Fig. 1. The LOLA OTA structure is made of optical-grade beryllium for its low mass, high stiffness, and high thermal conductivity. The OTA Main Housing serves as an optical bench for the Laser Transmitter and the Receiver Telescope. The Receiver Telescope is fiber-optic coupled to five Aft-Optics/Detector Assemblies mounted on the periphery of the Main Housing. A Reference Cube on the OTA is used to monitor laser to optical bench alignment during LOLA integration and environmental testing and to transfer the pointing angle of the LOLA Laser to the LRO spacecraft coordinate

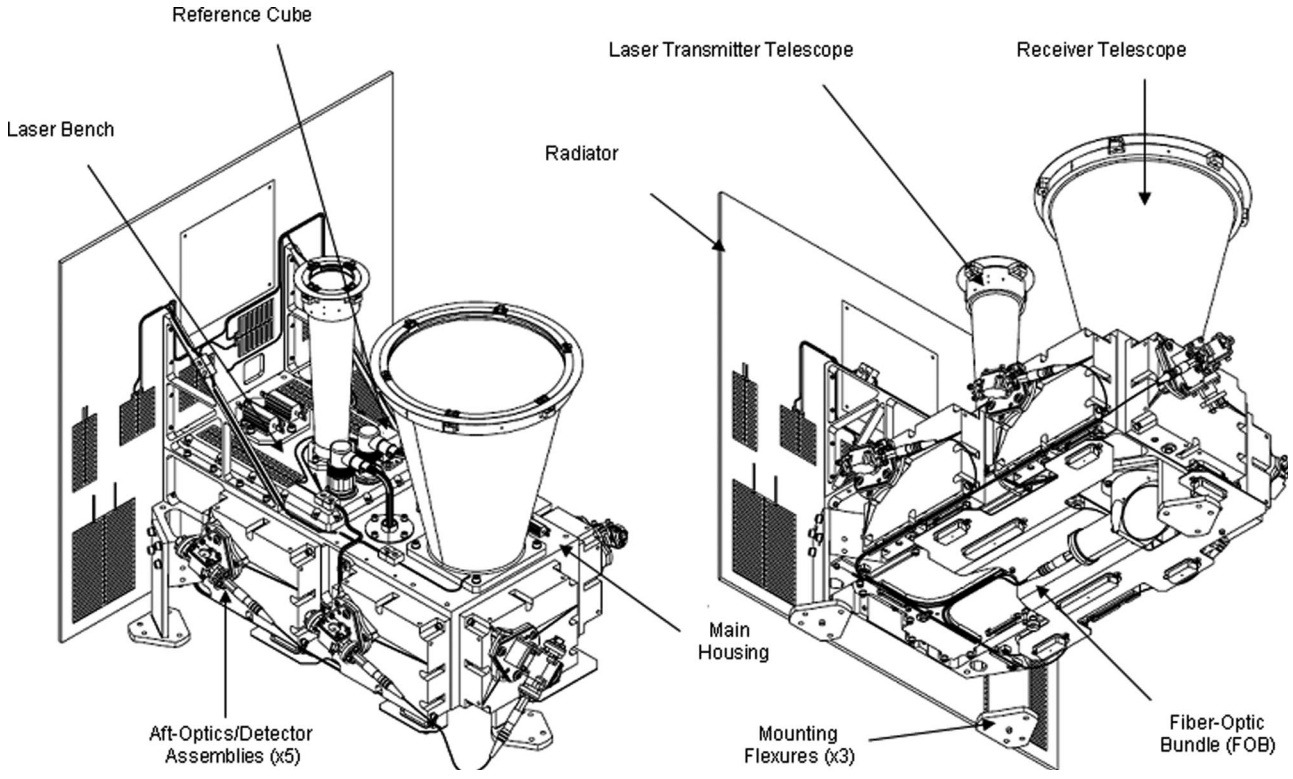

Fig. 1. LOLA Optical Transceiver Assembly (thermal blankets not shown).

system. The LOLA OTA is mounted to the LRO composite instrument deck via three titanium flexures, and the structure is fully enclosed by thermal blankets such that only the transmitter and receiver optical apertures and the radiator remain open to the external environment. Due to the Moon's harsh thermal environment, the LOLA optical system is required to operate over a wide temperature range, in a non steady state, and with large thermal gradients.

The LOLA Laser optomechanical design is similar to that of MLA: the laser is built on a small beryllium bench that mounts to the OTA Main Housing center compartment and has an external beam expander telescope that sets the final transmitted laser beam divergence. But while the MLA laser was a 20 mJ output energy oscillator/amplifier design, the LOLA laser has two independent oscillators to provide the required 2.7 mJ output energy with the lifetime and redundancy required by the LRO mission [5]. The two oscillator output beams are polarization coupled into a set of common optics that feed the external Laser Transmitter Telescope. At the top of this telescope is a diffractive optic element (DOE) that generates five far-field laser spots in a cross pattern. The four outer spots are separated by 500 μrad from the center spot, and the cross pattern is clocked by 26° with respect to the LRO spacecraft velocity vector to generate five equally spaced tracks on the lunar surface. The DOE is the key technology that allowed for the simple and elegant generation of the five LOLA Laser output beams.

The LOLA Receiver Telescope has a clear aperture (CA) diameter of 140 mm and is a scaled-up version of one of the 115 mm CA diameter MLA Receiver Telescopes. Both telescope designs have a 500 mm effective focal length (EFL) and use a 200 μm core diameter fiber optic to yield a receiver field-of-view (FOV) of 400 μm diameter. In the case of LOLA, five 200 μm fiber optics are mounted on a common connector located at the focal plane of the Receiver Telescope to obtain five independent FOVs coaligned with the five transmitted laser beams. The LOLA Fiber-Optic Bundle (FOB) fans out into five independent fiber-optic cables that attach to five Aft-Optics/Detector Assemblies where the fiber-optic output light is collimated, filtered, and imaged at a 1∶1 magnification onto each of the five 0.8 mm diameter Perkin-Elmer silicon avalanche photodiode (SiAPD) detectors. Unlike MLA, the LOLA receiver fiber-optic cables are not required to be the same length since any length difference (and hence range timing difference between the five channels) can be calibrated out. The LOLA FOB fan-out fiber-optic lengths were selected for optimum routing on the protective Delrin channels mounted on the underside of the OTA Main Housing.

The LOLA optomechanical design philosophy was the same we used on MLA: minimize the number of subassembly and instrument level adjustments required to align the instrument in order to better ensure alignment stability. All the LOLA optical and mechanical components were toleranced such that upon initial instrument integration the boresight error between the center laser beam and the center receiver telescope FOV was less than the ±2 mrad Receiver Telescope line-of-site (LOS) adjustment range. Like MLA, the LOLA boresight adjustment is implemented by decentering the fiber-optic adapter at the focal plane of the Receiver Telescope; but in the case of LOLA, this adapter also allows for clocking adjustment to optimize the tangential boresight alignment of the four outer channels. The radial boresight alignment of the four outer channels was accomplished by tolerancing the diffraction angle of the DOE, the focal length of the Receiver Telescope, and the position of the four outer fibers on the FOB common-end connector; no independent adjustment of the five Receiver Telescope FOV channels is possible because the fiber optics are closely packed and epoxied on the FOB common-end connector. Since LOLA's laser divergence and receiver channel FOV are similar to MLA's, we just modified MLA's instrument-level optical alignment requirements to include the alignment requirements for LOLA's four outer channels. LOLA's instrument-level alignment requirements are shown in Table 2.

3. Laser Transmitter Telescope

The LOLA laser transmitter telescope has two functions: it reduces the divergence of the LOLA laser oscillator input beam, and it splits the output beam into five to generate a cross pattern in the far-field. The telescope is an 18× magnification, afocal, Galilean beam expander that expands and collimates the LOLA laser 1 mm $1/e^2$ diameter, 1.8 mrad $1/e^2$ divergence input beam to generate the required 100 μrad $1/e^2$ diameter output beam divergence. The telescope has a single Corning 7980 fused silica negative lens, a BK7G18 positive lens group, and a DOE exit optic (Fig. 2). The DOE is a diffractive beam splitter that generates five output beams from a

Table 2. Lunar Orbiter Laser Altimeter Optical Alignment Requirements

Instrument integration	
Laser to receiver initial boresite error (center FOV)	<2 mrad
Laser perpendicular to LOLA mounting plane (center FOV)	<5 mrad
FOV pattern clocking with respect to LOLA instrument coordinates	26° ± 2°
Instrument alignment	
Laser to receiver boresite error (center FOV)	<20 μrad
Laser to receiver boresite error (edge FOV)	<40 μrad
Knowledge of laser beam(s) pointing with respect to S/C reference	±100 μrad
Instrument stability	
Laser pointing angle (relative to the LOLA mounting plane)	<150 μrad
Laser to receiver boresite error (all five beams)	<150 μrad

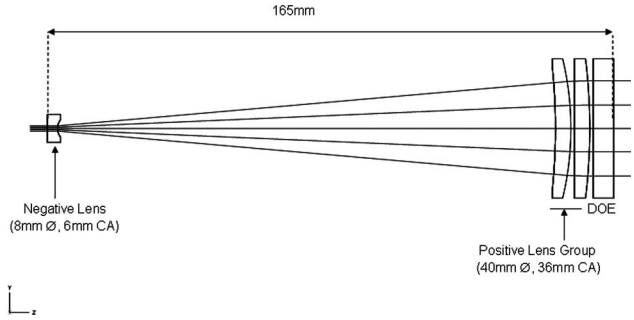

Fig. 2. LOLA Transmitter Telescope optical layout.

single input beam; this is an elegant beam splitting approach because it is simple, efficient, alignment insensitive (except for clocking), and environmentally insensitive [6]. The DOE optic is a 40 mm diameter by 6 mm thick fused silica substrate etched on one side with a transmission phase grating and antireflection (AR) coated on both sides to maximize transmission at 1064 nm. The LOLA DOE was manufactured by MEMS Optical from a master pattern that is replicated via a proprietary lithographic process onto a fused silica wafer from which multiple parts can be cored out. Before the final flight DOE was fabricated, several calibration wafers were made and tested to optimize the etch depth of the diffraction pattern in order to maximize efficiency and far-field beam uniformity. The flight DOE had an overall efficiency of 80% (the other 20% is diffracted to higher order modes outside the LOLA receiver FOV) with the center beam having ~50% more energy than each of the outer four beams. Figure 3 shows a picture of the DOE, its transmitted far-field image, and the far-field image normalized cross section in two orthogonal axes.

The telescope tube is beryllium with a titanium flexure preloaded to 30 lb (13.6 kg) in order to securely hold the positive lenses and DOE over all expected mechanical and thermal loads. The DOE and the tube mount both have semicircular notches, and a pin located in the flexure is used to provide a clocking lock feature between them. The negative lens is mounted on a titanium subcell whose axial location is shimmed to collimate the telescope for operation in vacuum at 1064 nm. The exit optics have a 36 mm diameter exit clear aperture (a 2:1 aperture to beam ratio) to prevent any significant vignetting of the output laser beam and allow for small decenter coalignment errors between the prime and the spare oscillator laser beams at the input to the Laser Transmitter Telescope. The LOLA Laser Transmitter Telescope was built using the same optomechanical tolerances, alignment requirements, and integration techniques that we used on the MLA 15× magnification laser transmitter telescope. The LOLA assembly, shown in Fig. 4(a), is 175 mm long, weighs 120 g, has an operational thermal range of 20 ± 20 °C, and a survival thermal range of −30 C to +70 °C. The expected solar background from the Moon into the LOLA Laser Transmitter Telescope is small and inconsequential to the operation of the LOLA Laser, due to its small aperture and small effective FOV. Two flight model (FM) Laser Transmitter Telescopes were integrated, functionally tested at ambient pressure and in a vacuum, thermally qualified for survival, and delivered to the LOLA laser team for integration to the Laser Bench.

4. Lunar Orbiter Laser Altimeter Receiver Telescope

The LOLA Receiver Telescope is a scaled up version of one of the MLA receiver telescopes. Both are 500 mm EFL telephoto designs, but the LOLA telescope has a larger diameter objective lens (150 mm versus 125 mm) and a longer unfolded path length to preserve the $f/2$ objective lens speed. MLA used a sapphire objective lens for its ability to survive in harsh thermal environments, but sapphire has the drawback of having a high density. To try to reduce mass we also designed, built, and tested an engineering model (EM) LOLA Receiver Telescope using a BK7G18 objective lens. The optical layout for both LOLA Receiver Telescope designs is shown in Fig. 5. The BK7G18 design has fewer elements because the objective lens is aspheric, and a single negative lens can set the final telescope EFL without the need to correct for the spherical aberration of the objective lens. The mass savings of this design were significant (220 g), and its defocus versus operating temperature negligible since BK7G18 has a

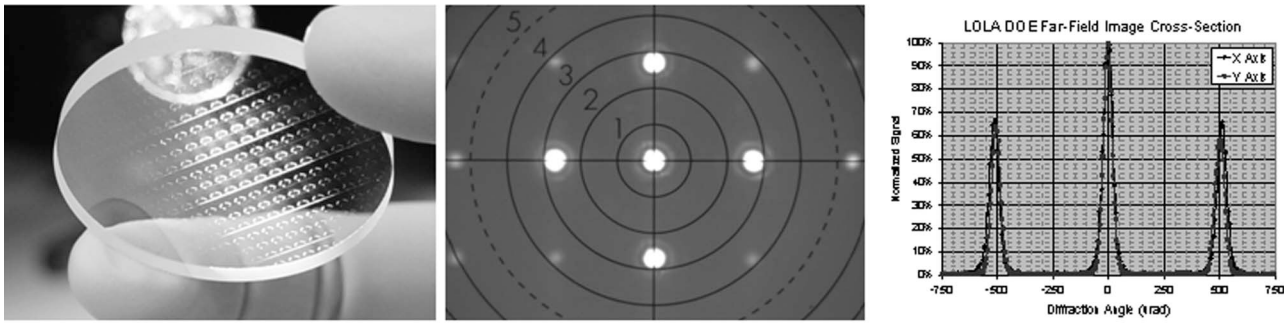

(a) (b) (c)

Fig. 3. (a) DOE, (b) far-field image (saturated), (c) image cross sections (normalized).

Fig. 4. (a) LOLA Transmitter Telescope, (b) LOLA Receiver Telescope.

dn/dT an order of magnitude smaller than sapphire, but the LOLA thermal model predicted that the BK7G18 objective lens would operate with large thermal gradients during orbit around the Moon due to the high emissivity and poor thermal conductivity of BK7G18. Figure 6 shows the predicted on-orbit temperatures for the two objective lens materials for the LRO Hot and Cold thermal cases; temperatures at the lens edge and lens internal and external center points are shown over a time period of three orbits. The sapphire objective lens operates over a temperature range of +11 °C to +42 °C with negligible thermal gradients, while the BK7G18 objective lens operates over a wider −24 °C to +56 °C temperature range and with radial and axial thermal gradients of up to 25 °C. The large and constantly changing thermal gradient would bend the BK7G18 objective lens back and forth during each LRO orbit. Although structural analysis and testing of the BK7G18 objective lens indicated that the lens would survive the predicted on-orbit thermal environment, we decided that it was safer to use the MLA-heritage telescope design for LOLA.

The LOLA Receiver Telescope optomechanical design is also based on MLA: the same materials (beryllium structure and titanium flexures), tolerances, optic mounting techniques, and alignment compensators for focus and boresight were used. The only change was the increased 250 lb (113.4 kg) flexure preload required to hold the larger LOLA objective lens. As in MLA, the telescope is folded with a dielectric mirror in order to fit within the allocated instrument volume and provide protection against an accidental view of the Sun that could otherwise damage the FOB located at its focal plane. The dielectric mirror reflects a small spectral band centered at 1064 nm and would allow most incident solar radiation to safely scatter off its frosted backside onto the LRO instrument deck. A picture of the LOLA Receiver Telescope is shown in Fig. 4(b). The assembly is 324 mm long and weighs 1.24 kg (driven mostly by the 680 g sapphire objective lens), has an operating temperature range of 20 ± 20 °C, and a survival temperature range of −30 °C to +70 °C. Two flight model (FM) Receiver Telescopes were integrated, functionally tested at ambient pressure and vacuum, thermally qualified for survival, and delivered to the LOLA mechanical team for integration to the OTA Main Bench.

The LOLA Receiver Telescope FOV is established by the FOB located at the telescope focal plane. The telescope side, or common end, of the FOB has five 200 μm core diameter, 0.22 NA, multimode, step-index fiber optics spaced 250 μm apart in a cross pattern; these fiber optics define five 400 μrad diameter FOVs with a center-to-center spacing of 500 μrad. The telescope FOB mating adapter is clocked 26° to align the five receiver FOVs with the five transmitted laser beams. Behind the common-end connector the FOB fans out into five independent fiber-optic cables that attach to the five Aft-Optics/Detector Assemblies. The LOLA FOB was fabricated in house at Goddard's Advanced Photonic Interconnection Manufacturing Laboratory/Code 562 [7]. The FOB is terminated with Diamond AVIM connectors, a space-qualified fiber-optic connector manufactured by Textron-Tempo Inc. and previously flown on the Geoscience Laser Altimeter System (GLAS) and MLA instruments. The FOB fan-outs have the standard version of this connector, while the FOB common-end has a customized internal ferrule capable of precisely locating and securing five fiber optics in a cross pattern. The fabrication of the modified common-end connector ferrule was a major part of the in-house FOB development effort. The Diamond AVIM connectors, together with the in-house fabricated mating adapters, allowed us to meet our stringent alignment requirements and provided the capability to mate and de-mate all fiber-optic interfaces without losing boresight alignment or

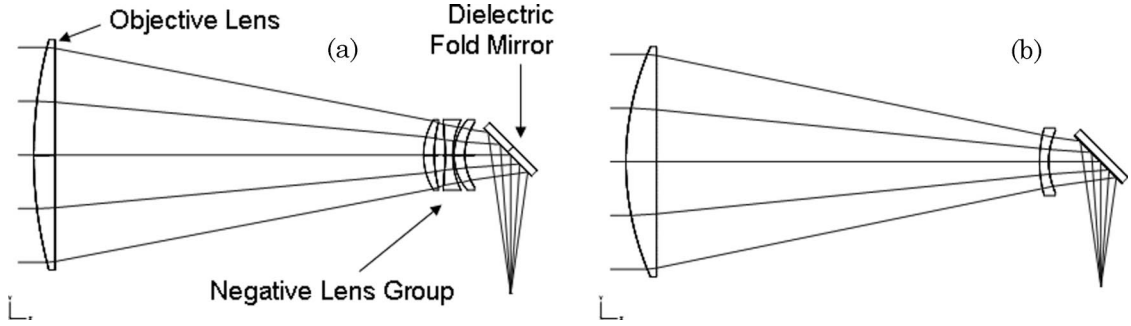

Fig. 5. LOLA Receiver Telescope layouts: (a) sapphire objective, (b) BK7G18 objective.

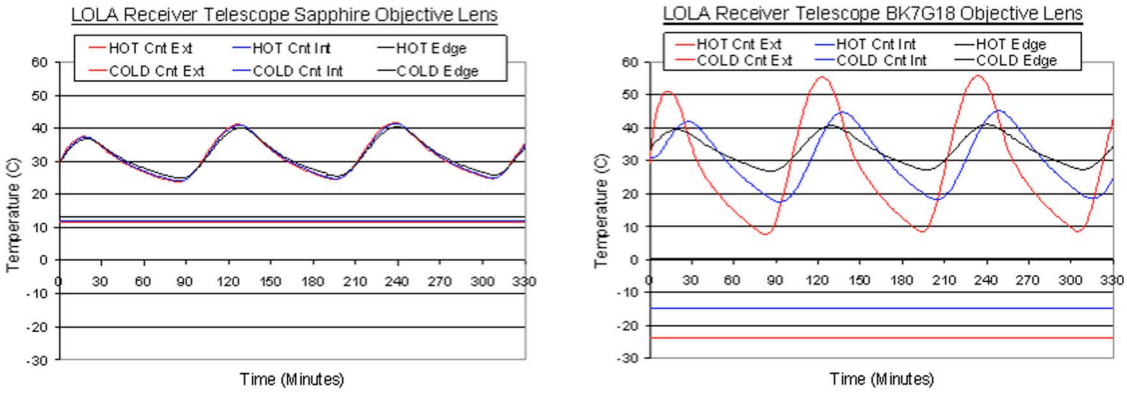

Fig. 6. (Color online) LOLA receiver objective lens on-orbit temperature: (a) sapphire, (b) BK7G18.

focus. After completion of the FOB assembly fabrication, all fiber-optic end faces were AR coated at 1064 nm by Denton Vacuum to increase the average fiber-optic transmission from ~90% to ~97%. The flight and flight spare FOB assemblies then underwent vacuum testing, operational and survival thermal testing, and vibration testing prior to delivery to the LOLA instrument integration and test (I&T). A picture of the LOLA FOB assembly and its common end is shown in Fig. 7.

Prior to installing the FOB on the LOLA OTA, the FOB was used to focus the Receiver Telescope and to measure the FOV and cross talk performance of the combined assembly. The Receiver Telescope/FOB interface allows for focus and boresight adjustments: focus is set by shimming the telescope FOB adapter and boresight by decentering the FOB adapter on the telescope mounting flange. The FOV of the combined LOLA Receiver Telescope and FOB can be measured two ways: (1) by back-illuminating the FOB and imaging the Receiver Telescope output, and (2) by scanning a point source at the focal plane of a collimator illuminating the receiver and plotting the output power of each FOB channel as a function of the source angular position. We used both methods during LOLA I&T and found them to be equivalent. Figure 8 shows the back-illuminated image of the combined LOLA Receiver Telescope/FOB assembly and two normalized FOV plots obtained with the second method described above. Note that the plots show that the FOV channels have the correct angular size (400 μrad FWHM) and center-to-center spacing (500 μrad). Plotting the multiple FOV cross sections on a log scale shows the amount of cross talk between the channels; our requirement is that the LOLA receiver system have <1% cross talk in order to not bias the five independent range measurements. The results shown in Fig. 8 were obtained with the telescope focus set for ambient pressure and were later verified with the telescope focus set for vacuum during the LOLA Thermal Vacuum (TVAC) test.

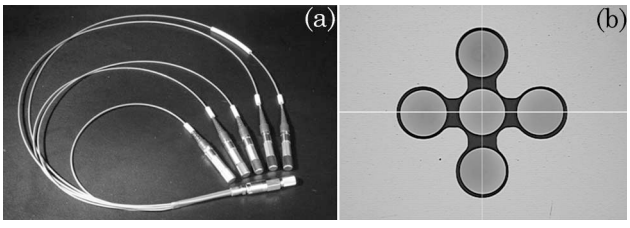

Fig. 7. LOLA fiber-optic bundle (FOB): (a) assembly, (b) common end.

The LOLA receiver system nominal FOV was selected to provide sufficient boresight alignment margin for each laser/receiver pair while having enough angular distance between neighboring channels to prevent cross talk. Cross talk is mainly a concern when environmental factors affect the receiver FOV size, the laser divergence, or the instrument boresight alignment; the first two can be caused by a telescope thermal defocus and the last one by a vibration induced telescope LOS shift. To prove that we met the cross talk requirement under different OTA alignment conditions, we made a set of four custom, calibrated, black and white Spectralon diffuse reflectance targets to measure the relative response of all five LOLA instrument channels. These 25 mm diameter targets were placed at the focal plane of a test collimator and illuminated by the LOLA laser while the signal from each LOLA Receiver FOV channel was monitored. The first target was all white with 99.3% reflectance at 1064 nm, and the second one was all black with 1.3% reflectance at 1064 nm. The other two targets had 1 mm diameter center inserts that subtended 400 μrad at the focal plane of our 2.5 m EFL test collimator; one target was white with a black insert, and the other one was black with a white insert. The worst-case cross talk target was the white target with the black insert; in this case the receiver center channel (CH1) collects little signal from its own laser and maximum cross talk from the four high-signal neighboring channels. We were able to show that with this worst-case target the CH1 cross talk signal met our <1% requirement even for cases where the boresight alignment error was as large as 150 μrad; we also showed that we met the cross talk requirement with the maximum expected on-orbit Receiver Telescope defocus. (For the cross

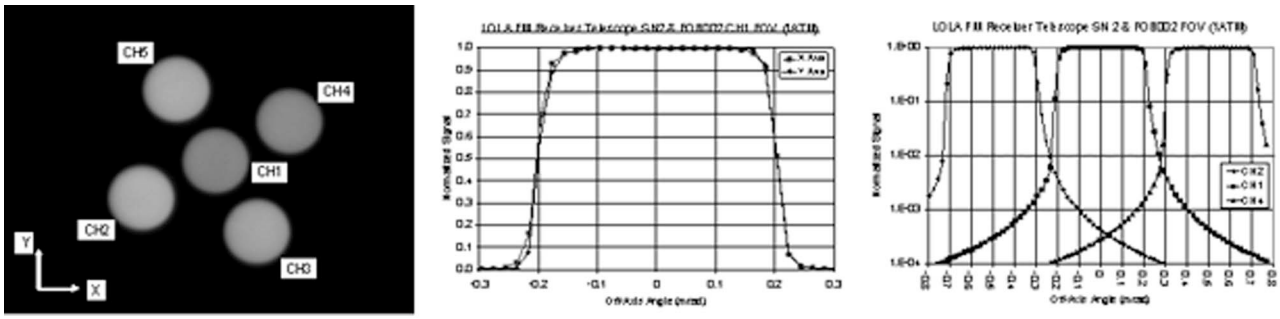

Fig. 8. LOLA receiver FOV: (a) Image, (b) CH1 FOV, (c) CH2-1-4 FOV (log scale).

talk test the Receiver Telescope focus was set for vacuum but operated at ambient pressure; the Receiver Telescope vacuum defocus just happens to be close to the expected worst-case on-orbit telescope thermal defocus, and it was easier to use pressure as opposed to temperature to change the telescope focal setting during the course of the cross talk test. The Laser Transmitter Telescope is also affected by pressure and temperature but not to the same extent as the Receiver Telescope due to its much slower f/#.)

5. Lunar Reconnaissance Orbiter Laser Ranging Telescope

LOLA was modified to allow for the measurement of an Earth-based laser ranging (LR) signal at 532 nm to help determine LRO's lunar orbit. A small Laser Ranging Telescope (LRT) located behind the LRO High Gain Antenna (HGA) will be illuminated by a pulsed laser source from NASA's Next Generation Satellite Laser Ranging (NGSLR) Station located at the GSFC in Greenbelt, Maryland, USA, and from International Laser Ranging Service (ILRS) sites around the globe. Laser ranging from the Earth to LRO can occur any time an Earth station is within the field of view of the LRT. The LRO HGA, with the coaligned LRT, will be pointed at White Sands, New Mexico for routine spacecraft communications whenever White Sands is in view. The signal collected by the LRT will be guided by a fiber-optic cable to the LOLA Aft-Optics/Detector Channel 1 (CH1) Assembly, where it will be detected and time stamped. CH1 was selected because this channel is aligned to the brightest of the five LOLA laser beams and has the highest signal-to-noise ratio (SNR). As such, CH1 can better handle the additional background noise generated when the LRT views a solar illuminated Earth. Nominally, the LOLA and Earth laser pulses will be timed to stagger their arrival on the LOLA CH1 detector; however, LOLA will also support asynchronous Earth ranging.

The derived LRT FOV requirement is 30 mrad diameter, which is wide enough to see Greenbelt, Maryland, when the LRO HGA is pointed at White Sands, New Mexico, and North America is normal to the Earth–Moon vector. The LRT aperture size is limited to 19 mm diameter by the etendue of the LOLA detector, which is defined as the product of the detector area and its illuminating cone solid angle. The LOLA SiAPD detector has a 0.7 mm diameter active area and can be illuminated at up to $f/1$ due to the size and location of the detector window. To conserve radiance, the product of the LRT aperture area and FOV solid angle cannot exceed the detector etendue. To bring the signal from the LRT to LOLA, a 10 m long fiber-optic cable is required. The cable is made of three mated segments to facilitate routing inside the two HGA gimbals, along the HGA boom, and across the spacecraft structure to LOLA. The LR fiber-optic cable is a bundle of seven, 400 μm core diameter, 0.22 NA, multimode, step-index, fiber optics in a 1.28 mm diameter hexpack configuration and is terminated using modified Diamond AVIM connectors [7]. This FOB design matches the LR optical system etendue, provides redundancy, and meets all bend radius routing requirements. The timing error introduced by using a 10 m, 0.22 NA, multimode fiber optic is only 0.4 ns, which can be calibrated during operations and accommodated in the LOLA science data analysis.

The LRT is a pupil imaging, afocal, 14.8× magnification, Keplerian telescope; the design images the telescope pupil onto the LR FOB to avoid generating a segmented FOV. An optical layout of the LRT is shown in Fig. 9. A sapphire objective lens images the Earth onto a field stop aperture that sets the LRT FOV, and a molded glass aspheric field lens located behind the field stop images the objective lens onto the LR FOB. The telescope design is folded with a 532 nm dielectric mirror to provide protection from an accidental view of the Sun and to facilitate routing of the LR FOB. A set of baffles mounted at the front of the telescope seals the gap to the HGA primary mirror 38.1 mm diameter aperture through which the LRT looks; the baffles also prevent direct illumination of the LRT objective lens for off-axis angles $>12°$. The LRT/Baffle Assembly can operate with the Sun as close to 5° off axis without exceeding the LOLA CH1 background noise generated when the LRT looks at a solar-illuminated Earth. The LRT objective lens and baffles are oversized to allow for ± 20 mrad adjustment of the LRT LOS, which is accomplished by decentering the field stop, field lens,

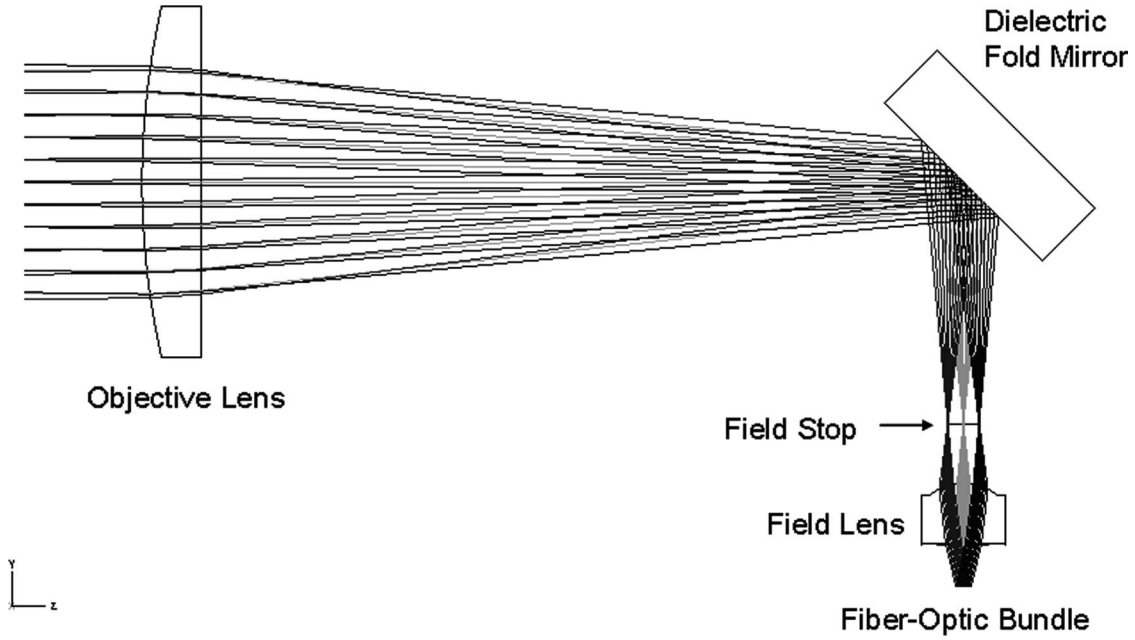

Fig. 9. LRO Laser Ranging Telescope (LRT) optical layout.

and FOB subassembly. The structure of the LRT is titanium to match the coefficient of thermal expansion (CTE) of the optical components given the harsh thermal environment expected on the HGA. A picture of the flight and flight spare LRT (with baffles) is shown in Figs. 10(a) and 10(b), which shows the LRT objective lens pupil image (the image of the back-illuminated LR FOB on the LRT objective lens), and Fig. 10(c) shows the measured LRT/LR FOB FOV cross section. The combined LRT/Baffle assembly is 225 mm long and weighs 348 g, and has an operating and survival temperature range requirement of 20 ± 30 °C and +90 °C to −40 °C, respectively. Prior to delivery to the HGA I&T team, the LRT was thermally qualified and vibration tested to 12.6 Grms for 1 minute on all three axes, without any significant change in its optical performance or LOS.

The LRT optical axis needs to be aligned parallel to the HGA RF axis; it is not possible to bias the two beams, one to look at GSFC while the other looks at White Sands, because the LRO orbit geometry and the viewed Earth phase change over time. The LRO HGA team used photogrammetric data from the antenna vendor as well as RF and optical measurements in the GSFC Electro-Magnetic Anechoic Chamber to determine the pointing angle of the HGA RF beam with respect to the HGA optical reference cube. We then used the HGA optical reference cube to align the LRT optical axis parallel to the HGA RF axis to within our allocated 0.36 mrad parallelism requirement. A picture of the HGA-LRT alignment setup is shown in Fig. 11. The pointing angle of the LRT optical axis relative to the HGA optical reference cube was monitored during the HGA/Boom Assembly vibration and thermal vacuum (TVAC) tests, and the LRT alignment stayed within our allocated pointing angle requirement. In addition to the alignment tests, the 532 nm transmission of the LRT and LR FOB system was measured before and after each HGA environmental test. The completed HGA/Boom Assembly was mated to LRO, and the final LR FOB segment was routed from the bottom of the

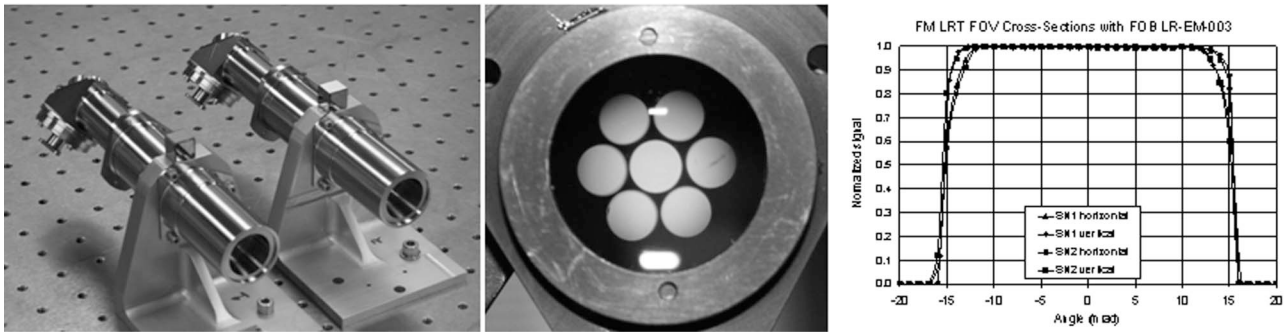

(a) (b) (c)

Fig. 10. (a) LRO Laser Ranging Telescopes, (b) pupil image, (c) FOV image cross sections.

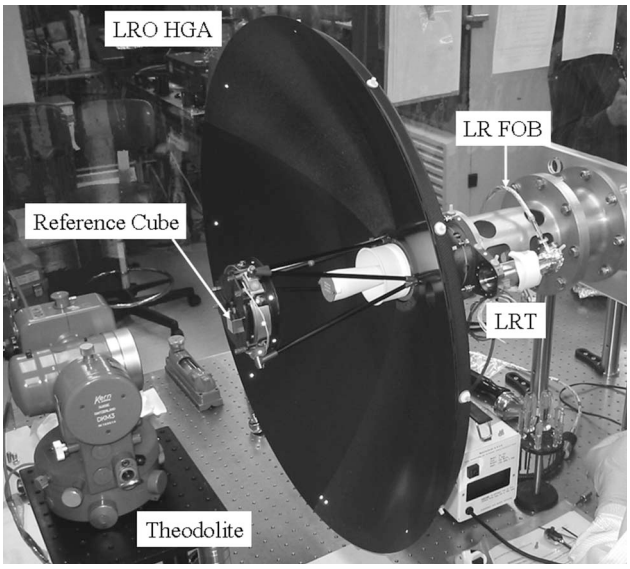

Fig. 11. LRO HGA-LRT alignment setup.

HGA boom to the LOLA CH1 Aft-Optics LR FOB input port. After integration, the LR Flight System end-to-end performance was tested with simulated 532 nm and 1064 nm pulsed and CW signals going into the LOLA Receiver Telescope and LTR to mimic the expected Lunar and Earth laser ranging signals and solar background levels.

6. Aft-Optics Assemblies

The five LOLA Aft-Optics Assemblies have two different optical designs: the Channel 1 (CH1) assembly operates at 1064 nm and 532 nm to handle the LOLA center FOV and LRT input signals, while the other four Aft-Optics assemblies (CH2–CH5) operate at 1064 nm only and view the signals from the four outer LOLA FOV channels. The function of the Aft-Optics is to collimate, filter, and reimage the LOLA and LRT receiver fiber optic onto the five LOLA 0.8 mm diameter SiAPD detectors. The CH2—CH5 Aft-Optics design has 11 mm EFL, $f/2$ Lightpath molded aspheric lenses to collimate and refocus the 200 μm diameter LOLA fiber optic at a 1:1 magnification; this lens EFL provides the <20 mrad collimated beam divergence required for the LOLA 2 cavity, 1064.45 nm center wavelength, 0.7 nm FWHM bandpass filter made by Barr Associates. The CH1 Aft-Optics design has the same 1064 nm collimating lens and bandpass filter, but includes a dichroic beam splitter and larger 532 nm collimating and detector refocusing lenses to handle the larger 1.28 mm diameter LRT FOB input. The LR filter is also from Barr Associates; it has a center wavelength of 532.25 nm, but it is only 0.3 nm FWHM to reduce the large solar background expected when the LRT views the Earth in daylight. Both filters were purchased with center wavelengths longer than their respective laser wavelengths in order to tilt-tune the filters to optimize their transmission. The bandpass of the filters shifts to a lower wavelength as the angle of incidence (AOI) increases; we determined the optimum AOI for each filter by measuring their transmission as a function of AOI using a collimated, attenuated beam from the LOLA FM laser and the prime and spare LR ground lasers. The Aft-Optics optomechanical design allows for up to a 3° off-normal angle of incidence (AOI) on the bandpass filters, which was twice our expected optimum filter AOI. The optical layout for both Aft-Optics designs is shown in Fig. 12.

Both Aft-Optics designs include a 1064 nm test port that serves two purposes: it allows for the back-illumination of the LOLA FOB so we can view and monitor the LOLA Receiver FOV and LOS alignment during I&T, and it allows for the input of five different signal and background levels that can simulate lunar returns for testing the receiver detectors, electronics, and signal processing algorithms. The addition of the test port complicated the optomechanical design and alignment of the Aft-Optics assemblies, but proved very useful during instrument-level functional and environmental testing. The test port is implemented with a 99%R/1%T 1064 nm power beam splitter with a mirrored common surface to split the signal from the test port fiber optic to the receiver fiber optic and to the detector focal plane. Shimming the power beam splitter with a wedged spacer changed the angle of incidence of the collimated beam on the 1064 nm bandpass filter in order to tilt-tune the filter to its predetermined optimum

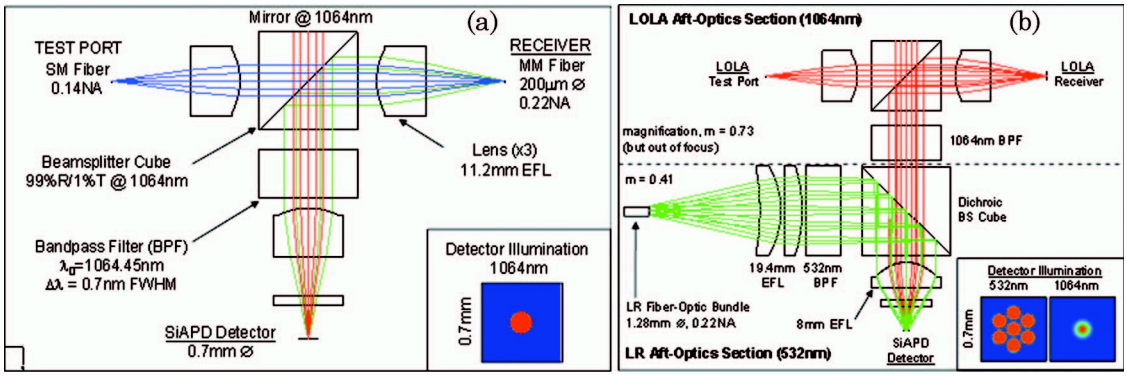

Fig. 12. LOLA Aft-Optics optical layouts: (a) CH2—CH5, (b) CH 1 (1064/532 nm).

AOI. Tilt-tuning the LR channel was accomplished by decentering the LR FOB Aft-Optics connector to change the AOI of the collimated beam on the 532 nm filter. The CH1 Aft-Optics design allows for different AOIs on the 1064 nm and 532 nm filters with coincident 1064 nm and 532 nm images on the detector focal plane since rotating the dichroic beam splitter cube moves the 532 nm focal plane image without affecting the location of the 1064 nm image. The only catch is that both filter tilt-tune adjustments have to be made in the same plane as the dichroic beam splitter rotation provides adjustment in.

A picture of two LOLA Aft-Optics Assemblies is shown in Fig. 13. The CH1 design weighs 97 g while the smaller CH2—CH5 design is only 44.6 g. Both designs have an operational thermal range of 20 °C ± 20 °C and a survival thermal range of −30 °C to +50 °C. The mechanical components are titanium to match the CTE of the optics and the beam splitters are bonded with Scotch-Weld 2216 Grey epoxy. Thermal defocus and beam decollimation over the thermal operating range is small and can be neglected. The Aft-Optics can also be aligned at ambient pressure and operated in vacuum without requiring defocus compensation since the change in collimation and imaging with pressure is negligible. The Aft-Optics Assemblies mate to the beryllium detector housings via a titanium interface plate that allows for focus and decenter adjustment; the SiAPD detectors have the same thermal operating range as the Aft-Optics Assemblies so the interface does not need to provide thermal isolation. The Aft-Optics Assemblies are aligned to the LOLA detectors by looking through the Aft-Optics LOLA receiver fiber-optic input port to focus and center the detector image on the FOB adapter aperture (we had previously verified that the LOLA receiver fiber optic was well centered on its connector, that the connector was well centered on its adapter, that the test port fiber optic was aligned to the receiver port fiber optic, and that the images from the 1064 nm and 532 nm input fiber optics were coincident on the CH1 Aft-Optics focal plane). The LOLA Aft-Optics/Detector alignment optical setup is shown in Fig. 14; the inset images

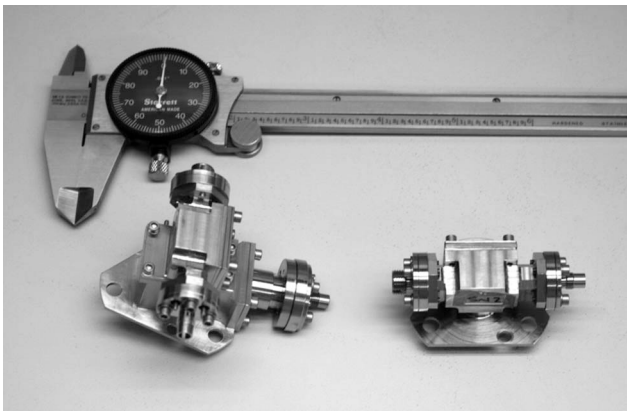

Fig. 13. LOLA Aft-Optics assemblies: CH1 (left), CH2—CH5 (right).

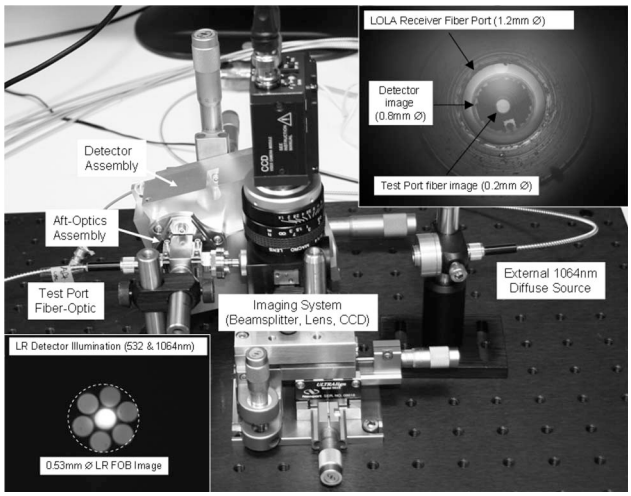

Fig. 14. LOLA Aft-Optics/Detector Assembly alignment setup and images (insets).

show the alignment of the detector to the LOLA receiver port and the coalignment of the 1064/532 nm fiber-optics images on the CH1 Aft-Optics assembly focal plane. After the Aft-Optics/Detector alignment was completed, the Aft-Optics fiber-optic adapters and the detector interface plate were "liquid pinned" (epoxy applied to a mounting flange pin aligned to an oversized hole on the mating flange) with Scotch-Weld 2216 Grey epoxy. The mated Aft-Optics/Detector Assemblies were then installed on the OTA Main Housing and electrically integrated to the detector power supply and signal processing electronics.

We performed a radiometric end-to-end test of the LOLA and LR receiver optical systems using the LOLA and LR Receiver Telescopes, Fiber-Optic Bundles, and Aft-Optics Assemblies. The goal of the test was to verify that the radiometric performance of the receivers was close to theoretical given their respective aperture, FOV, filter spectral bandwidth, and measured optical component transmissions. The test consisted of measuring the LOLA and LR receiver system output power as a function of distance to the 10 in. diameter exit port of the NASA/GSFC Code 614.4 calibration group's 36 in. diameter integrating sphere (Fig. 15). Since the integrating sphere exit port is an extended white light source (akin to a solar illuminated Moon) when viewed up close, this test also verified that the off-axis and out-of-band transmission of both receiver systems was adequate and met the background noise assumptions that went into both laser ranging link margin calculations. Using the calibrated spectral radiance of the sphere exit port at 532 nm and 1064 nm, we calculated that the LOLA and LR receiver systems should collect 1.0 nW and 7.0 nW, respectively. The LR receiver system collected ~10% more power than calculated and was insensitive to distance over a 0.3 m to 6.1 m range (the long dimension being limited by the size of the clean room). The LOLA receiver system collected 50–70% more power than calculated

Fig. 15. LOLA and LR receiver systems radiometric test setup.

depending on sphere distance; this performance was similar to what we had measured on MLA and was taken into account in the initial LOLA link margin calculation. The actual versus theoretical discrepancy is because the theoretical calculation assumes an ideal bandpass filter with no transmission outside its bandpass and an ideal telescope with zero transmission outside its FOV. We believe that the LR receiver system performance was closer to theoretical and insensitive to distance because the LRT has a set of baffles that limit the off-axis illumination of its objective lens. Instrument volume constraints precluded the use of baffles to limit the off-axis illumination of the LOLA Receiver Telescope objective lens.

7. Lunar Orbiter Laser Altimeter Optical Transceiver Assembly Optical Integration

The development of the LOLA optical system included building and testing engineering model (EM) copies of each optical assembly and integrating and testing an EM OTA. The EM optical assemblies had the same optical components as the flight model (FM) assemblies, but used aluminum instead of titanium or beryllium for the structural components. Integrating and testing EM assemblies early in the instrument development program is critical to correct any design flaws, verify all optomechanical interfaces, draft documentation and optical test procedures, and identify all required optical Ground Support Equipment (GSE). All the LOLA optical flight model (FM) assemblies were space qualified per GSFC-STD-7000 General Environmental Verification Specification (GEVS) guidelines; functional tests were performed before and after each environmental test. The environmental tests included operational and survival thermal testing, operation in vacuum, and vibration testing of the LRT and the Laser/Beam Expander Assembly. The FM OTA optomechanical integration was straightforward: the optical assemblies were bolted to the OTA Main Housing and the LOLA FOB was integrated to the Receiver Telescope and to the five Aft-Optics Assemblies. Routing and securing the LOLA FOB to the Delrin channels on the underside of the Main Housing was the only difficult task due to the bend radius

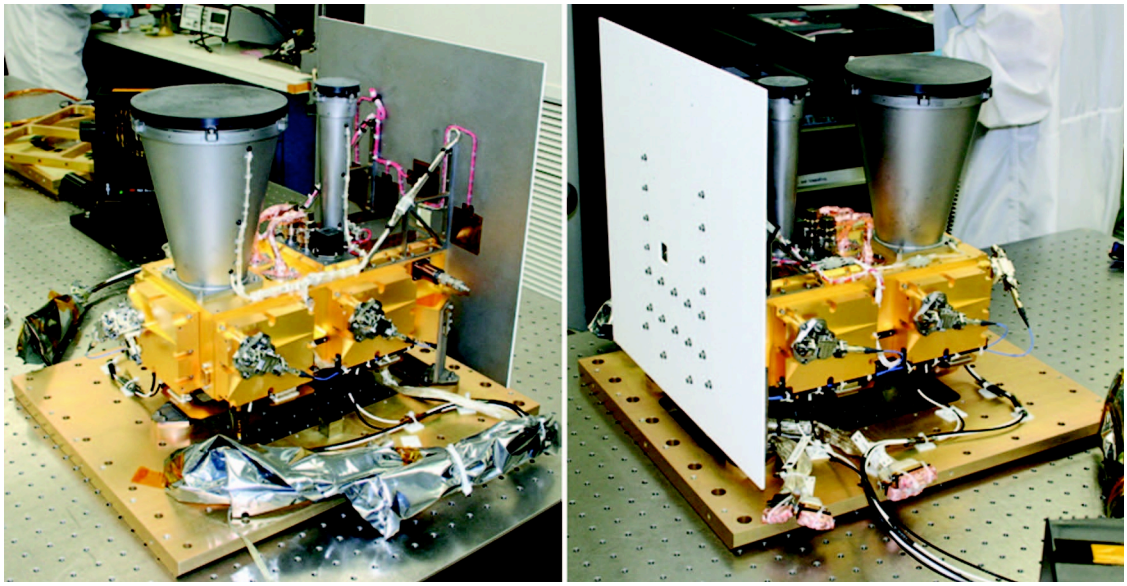

Fig. 16. LOLA FM OTA (thermal blankets not shown).

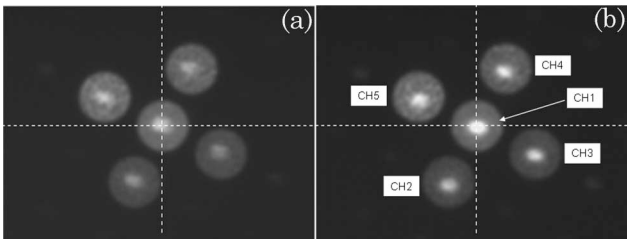

Fig. 17. LOLA OTA initial boresite alignment: (a) Laser 1, (b) Laser 2.

constraints of the FOB. The integrated LOLA FM OTA is shown in Fig. 16.

Two optical alignment activities completed the optical integration of the FM OTA: the boresight alignment of the transmitter and receiver and the measurement of the pointing angle of the five transmitted laser beams with respect to the LOLA reference cube. The LOLA boresight alignment procedure and test setup were the same as used on MLA. To boresight the OTA, the Laser output beam is attenuated and viewed with a CCD camera located at the focal plane of a 2.5 m EFL collimator, the LOLA FOB is back-illuminated, and the Receiver Telescope FOB adapter is decentered and rotated until the images of the receiver five FOVs are centered on the five transmitted laser beams. After final OTA boresight alignment, the Receiver Telescope FOB adapter was locked in place with four fasteners and "liquid pinned" and the FOB connector "torque striped" to its adapter with a dab of epoxy. Figure 17 shows the initial boresight alignment images for both LOLA Laser oscillators. On these images the receiver FOV image is in-focus because we back-illuminated at 1038 nm to compensate for the LOLA Receiver Telescope defocus at ambient pressure. The laser images are ~1.5× larger than what we expect in vacuum due to the pressure defocus of the Laser Transmitter Telescope. Note also that the two LOLA laser oscillators do not point in exactly the same direction (they are ~35 μrad off in the vertical axis), which required a compromise in the OTA boresight alignment. The measurement of the LOLA Laser pointing angle relative to the LOLA Reference Cube was accomplished with an autocollimating theodolite that "aperture shared" the laser output beam and the LOLA Reference Cube and measured the orientation of the five transmitted laser beams relative to the reference cube $+Z$ face (the theodolite reticule was viewed with a CCD camera in order to see the LOLA IR laser beams). This measurement was later used to transfer the LOLA Laser pointing angle information to the LRO spacecraft coordinate system.

The completed LOLA OTA underwent sine, random, and sine burst vibration testing to proto-flight levels. The plan called for a sine burst test level of 11.2 Grms about all three axes, but a failure of the vibration table during the Z-axis test led to an overtest condition of nearly a factor of 2. Although the structural margin of safety remained positive, we did see a significant boresight alignment shift after this test. The Z-axis vibration test was later completed at another facility, and this time the OTA boresight alignment remained stable. Figure 18 summarizes the OTA vibration test alignment results; the left plot shows the pointing angle stability of the LOLA Laser center beam versus the LOLA Reference Cube, while the right plot shows the boresight alignment of both lasers to the receiver. Included in the plots are circles denoting the angular size of the LOLA Receiver FOV, as well as our allocated budget for allowable alignment shifts during the LOLA and LRO spacecraft (S/C) level environmental test programs. Two things to note on these plots: (1) the pointing shift of the LOLA Laser was small and within allocation, and (2) the OTA boresight alignment error was mostly due to a change in the Receiver Telescope LOS and was near the limit of our S/C-level allocated error budget. The need to

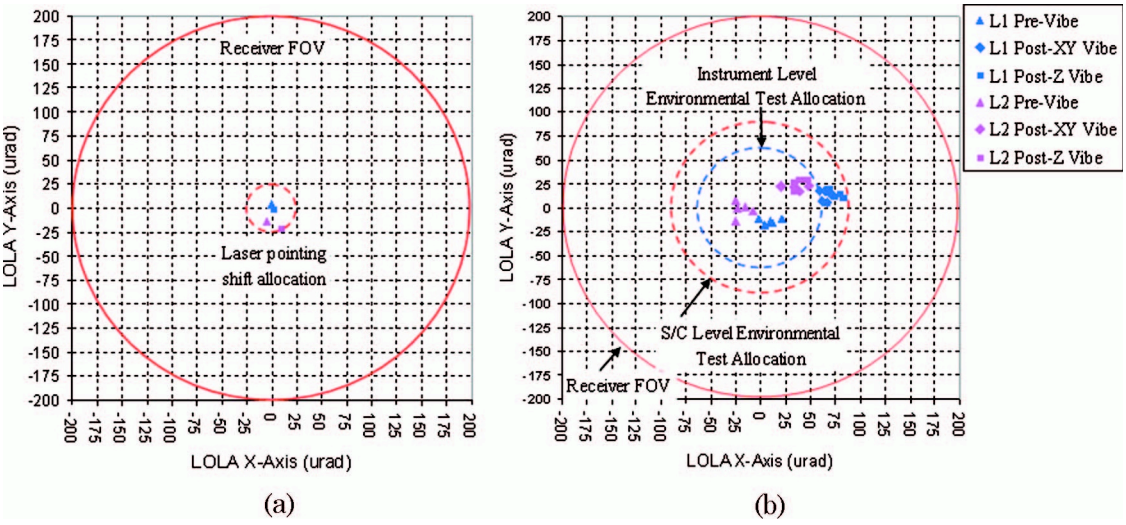

Fig. 18. LOLA OTA pre- and post-vibe alignment: (a) laser, (b) boresight.

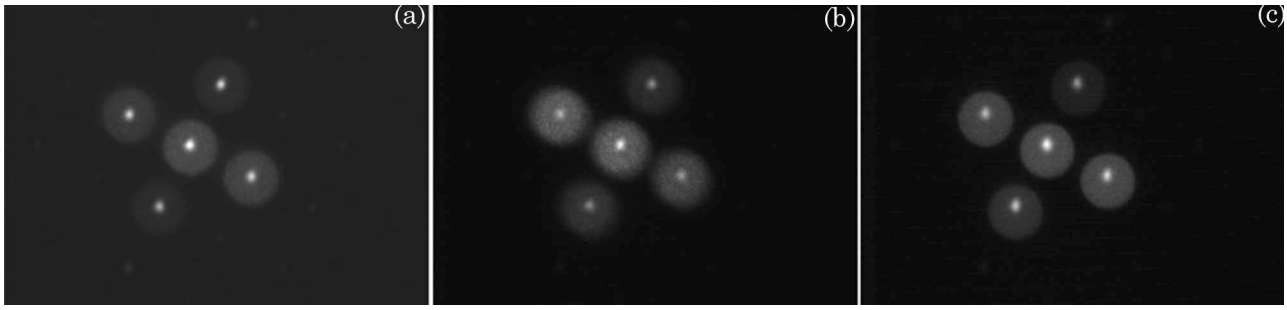

Fig. 19. LOLA Laser 2 TVAC boresite alignment: (a) ambient, (b) hot qual., (c) cold qual.

replace an electronic component in the Main Electronics Box (MEB) at the beginning of the LOLA instrument-level thermal vacuum (TVAC) test gave us the opportunity to reboresight the OTA.

The LOLA TVAC test lasted several weeks and included eight hot and cold cycles that encompassed LOLA's survival and operational thermal ranges. For the TVAC test the LOLA OTA was fully blanketed, mounted horizontally, and pointed at the TVAC chamber optical window so we could monitor the alignment of the LOLA OTA with an external collimator/CCD camera system. During the TVAC test the LOLA Laser was attenuated by the Laser Beam Dump (LBD), an MLA heritage optical GSE device that attenuates the laser without changing its pointing angle or divergence, and the beam enclosed by a tube that went all the way to the TVAC chamber window to prevent scatter or ghost reflections from illuminating the LOLA Receiver Telescope and saturating or damaging the sensitive LOLA detectors. At the same time the Receiver Telescope fiber optics were back-illuminated at 1061 nm via the Aft-Optics test ports; we did not back-illuminate at 1064 nm to prevent saturating the LOLA detectors (1061 nm is close enough to get an in-focus Receiver Telescope image in vacuum, but far enough from the LOLA bandpass filter center wavelength to provide sufficient attenuation in the Aft-Optics). Finally, an external laser source was used to illuminate the LOLA Reference Cube such that we could see on the external collimator CCD a far-field image of the LOLA Laser, the LOLA Receiver FOV, and the LOLA Reference Cube $+Z$ face. The LOLA Laser pointing angle and divergence and the OTA boresight alignment were very stable during the course of the TVAC test. Figure 19 shows three representative boresight alignment images for different portions of the LOLA TVAC test profile. Note the smaller size of the laser far-field image when the instrument operates in vacuum; also note that, as expected, the LOLA Receiver Telescope FOV gets slightly out of focus at the 36 °C HOT Qual operating temperature. After completion of the TVAC test, LOLA underwent a complete functional checkout and was delivered to LRO for integration to the spacecraft.

8. Lunar Orbiter Laser Altimeter Integration to Lunar Reconnaissance Orbiter

LOLA was delivered to the NASA/GSFC Lunar Reconnaissance Orbiter (LRO) spacecraft I&T team on April 2008 and integrated onto the spacecraft on May 2008. A photo of LOLA integrated to the LRO instrument deck, and with thermal blankets installed, is shown in Fig. 20. The LOLA OTA was integrated to the LRO instrument deck without any need for active alignment (i.e., without the need to shim the three flexure interfaces) to meet our coalignment requirement to the Lunar Reconnaissance Orbiter Camera (LROC) instrument. The OTA was designed to meet a <5 mrad perpendicularity error requirement between the LOLA Laser center output beam and the LOLA mounting plane defined by the

Fig. 20. LOLA integrated to the LRO spacecraft.

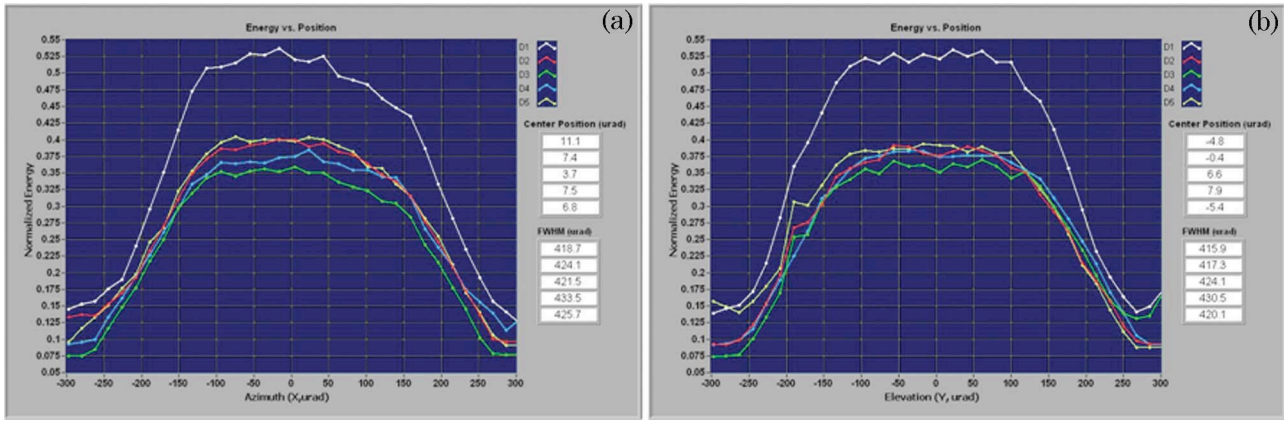

Fig. 21. (Color online) LOLA Laser 1 S/C level boresite alignment: (a) X axis, (b) Y axis.

three mounting flexures. The pointing angle of the LOLA Reference Cube with respect to the LRO Master Reference Cube was measured and documented, and the pointing angle of the five transmitted LOLA laser beams with respect to the LRO Star Tracker optical axis was established. After the LRO HGA with the integrated LR system was installed on LRO, the LR FOB Segment 3 was mated to the LOLA Aft-Optics CH1 LRT input port and an end-to-end LR system test was performed. Full functional tests of the LOLA and LR optical systems, including measuring the OTA boresight alignment and the alignment of the LRT to the HGA reference cube, were performed before and after each LRO environmental test.

The collimator system used during LOLA I&T and TVAC test to monitor the instrument alignment was too large and cumbersome to use for the LOLA S/C-level alignment tests, so the MLA-heritage LTR/Risley Target Assembly was reconfigured for LOLA use. This target includes a tube that attaches to the LOLA Laser Transmitter Telescope and fully encloses the LOLA laser beam, the Laser Beam Dump (LBD) to attenuate the laser energy, a Lateral Transfer Retroreflector (LTR) to send the LOLA laser beam back into the LOLA Receiver Telescope aperture, and a set of motorized Risley prisms to deviate the retroreflected laser beam in two orthogonal axes over a $\pm 650\,\mu$rad range. The LTR is a hollow cube-corner section comprised of a flat mirror and a roof mirror assembly that translates and flips the input laser beam by 180°; the device is alignment insensitive and was manufactured by PLX Inc. to an accuracy of <2 arcseconds ($<10\,\mu$rad). The function of the LTR/Risley Target Assembly is to scan the LOLA Laser far-field image across the LOLA Receiver Telescope focal plane in order to generate cross-sectional plots of the receiver FOV and to determine the boresight error of each of the five transmitted beams with respect to their corresponding receiver channels. Figure 21 shows the results obtained after LOLA integration to LRO for the LOLA Laser 1 oscillator. The boresight error for every channel was $<11\,\mu$rad and was obtained from the cross-sectional FOV plot center offset; the shape of the FOV cross sections were not top-hat, and the measured FWHM was slightly larger than the nominal $400\,\mu$rad receiver FOV because the test was conducted at ambient pressure with both the LOLA Transmitter Telescope and the LOLA Receiver Telescope out of focus. As expected, the CH1 curve was $\sim 50\%$ higher than the rest because the laser center beam has more energy. We repeated this test after the LRO vibration test and after the LRO TVAC test without observing any significant shift in LOLA's boresight alignment. The test was repeated one final time after the fully-integrated LRO spacecraft arrived at the Astrotech processing facility near the Cape Canaveral Air Force Station launch site in Florida, and LOLA's boresight alignment was still stable and within allocation. We also measured no change in the alignment of the LRT with respect to the HGA reference cube during the course of the LRO environmental test program and one final time at Astrotech.

9. Conclusion

This paper presented the optical system design, optical integration, and optical test results for the LOLA instrument, a multichannel laser altimeter recently developed at NASA's GSFC. LOLA incorporates novel optical technologies such as a diffractive optic element to generate multiple transmitted laser beams, a fiber-optic bundle to generate multiple receiver FOVs aligned to the multiple transmitted laser beams, a test port on the Aft-Optics/Detector assemblies to facilitate instrument alignment and testing, and a laser ranging (LR) system capable of improving the orbit determination of LRO around the Moon. LOLA instrument-level integration and testing was completed on April 2008, and LRO spacecraft-level integration and environmental testing was completed on December 2008. During both the instrument and the spacecraft level functional and environmental test programs, LOLA performed well and met all of its optical design requirements. As of this writing, the LRO spacecraft is undergoing final checkouts at the Astrotech facility in Florida. LRO is

scheduled to launch aboard an Atlas V rocket on June 2009 for its five day ride to the Moon.

The work presented in this paper would not have been possible without the contributions of many other individuals at NASA/GSFC. In particular we would like to thank Mr. Clarence (Sid) Johnson, Dr. Danny Krebs, Dr. Anne Marie Novo-Gradac, Dr. Anthony Yu, Dr. George Shaw, Ms. Melanie Ott, Mr. Rob Switzer, Mr. Joe Thomas, Mr. Adam Matuszeski, Mr. Keith Cleveland, Dr. Xiaoli Sun, Mr. Rob Taminelli, Mr. Jay Smith, Mr. Ron Zellar, Mr. Craig Coltharp, and Mr. Glenn Jackson.

References

1. G. Chin, S. Brylow, M. Foote, J. Garvin, J. Kasper, J. Keller, M. Litvak, I. Mitrofanov, D. Paige, K. Raney, M. Robinson, A. Sanin, D. Smith, H. Spence, P. Spudis, S. A. Stern, and M. Zuber, "Lunar Reconnaissance Orbiter overview: the instrument suite and mission," Space Sci. Rev. **129**, 391–419 (2007).
2. D. E. Smith, M. T. Zuber, G. B. Jackson, J. F. Cavanaugh, G. A. Neumann, H. Riris, X. Sun, R. S. Zellar, C. Coltharp, J. Connelly, R. B. Katz, I. Kleyner, P. Liiva, A. Matuszeski, E. Mazarico, J. F. McGarry, A. M. Novo-Gradac, M. N. Ott, C. Peters, L. A. Ramos-Izquierdo, M. H. Torrence, E. Mazarico, J. Connelly, D. D. Rowlands, T. Zagwodzki, L. Ramsey, D. D. Rowlands, S. Schmidt, V. S. Scott III, G. B. Shaw, J. C. Smith, J.-P. Swinski, M. H. Torrence, G. Unger, A. W. Yu, and T. W. Zagwodzki, "The Lunar Orbiter Laser Altimeter investigation on the Lunar Orbiter Reconnaissance mission," Space Sci. Rev. (to be published).
3. L. Ramos-Izquierdo, V. S. Scott III, S. Schmidt, J. Britt, W. Mamakos, R. Trunzo, J. Cavanaugh, and R. Miller, "Optical system design and integration of the Mercury Laser Altimeter," Appl. Opt. **44**, 1748–1760 (2005).
4. H. Riris, X. Sun, J. F. Cavanaugh, G. B. Jackson, L. Ramos-Izquierdo, D. E. Smith, and M. Zuber, "The Lunar Orbiter Laser Altimeter (LOLA) on NASA's Lunar Reconnaissance Orbiter (LRO) Mission," Proc. SPIE **6555**, 65550I (2007).
5. A. W. Yu, A. M. Novo-Gradac, G. B. Shaw, G. Unger, L. Ramos-Izquierdo, and A. Lukemire, "The Lunar Orbiter Laser Altimeter (LOLA) Laser Transmitter," Proc. SPIE **6871**, 68710D (2008).
6. J. G. Smith, L. Ramos-Izquierdo, A. Stockham, and S. Scott, "Diffractive optics for moon topography mapping," Proc. SPIE **6223**, 622304 (2006).
7. M. N. Ott, R. Switzer, R. Chuska, F. LaRocca, W. J. Thomes, and S. MacMurphy, "Development, qualification and integration of the optical fiber array assemblies for the Lunar Reconnaissance Orbiter," Proc. SPIE **7095**, 70750P (2008).